Photocatalytic Oxidation of Nitrobenzene and Phenylamine: Pathways and Kinetics

Giovanni Palmisano, Vittorio Loddo, Vincenzo Augugliaro, and Leonardo Palmisano
Dipartimento di Ingegneria Chimica dei Processi e dei Materiali, Università di Palermo, Viale delle Scienze, 90128 Palermo, Italy

Sedat Yurdakal
Kimya Bölümü, Fen Fakültesi Anadolu Üniversitesi, Yunus Emre Kampüsü, 26470 Eskişehir, Turkey

DOI 10.1002/aic.11137
Published online February 27, 2007 in Wiley InterScience (www.interscience.wiley.com).

The oxidation of nitrobenzene and phenylamine has been carried out by heterogeneous photocatalysis in aqueous suspensions of commercial TiO_2. The photoreactivity results indicate that two reaction pathways occur in parallel with both substrates from the start of irradiation: partial oxidation to monohydroxy derivatives and mineralization. The first pathway involves the entering of radical $HO^{\bullet}$ into the aromatic ring giving rise to monohydroxy derivatives, and the second one involves the total oxidation of the substrates to CO_2. The partial oxidation of nitrobenzene produces all the three possible monohydroxy derivatives, while that of phenylamine only produces the ortho- *and* para-*isomers. The extent of adsorption in the dark was found to be about 8% mol for nitrobenzene, while the amounts were not detectable for phenylamine. The Langmuir-Hinshelwood approach has been satisfactorily applied for modeling the photoreactivity results, and the values of the kinetic model parameters have been determined.* © 2007 American Institute of Chemical Engineers *AIChE J,* 53: 961–968, 2007
Keywords: partial oxidation, nitrobenzene, phenylamine, heterogeneous photocatalysis, reaction pathway, kinetics, TiO_2

Introduction

Heterogeneous photocatalysis in the presence of semiconductor materials[1–4] is an advanced oxidation process developed in these last years. This new method has shown to be effective for the oxidation of a lot of organic and inorganic compounds in mild conditions of temperature, and pressure with a measurable rate up to negligible concentration levels. Among its relevant applications[5–7] the main one is related to the degradation of environmental pollutants present in water or air.

The basic principles of heterogeneous photocatalysis are well established. When a photon with an energy of hν (h, Planck constant and ν, wave number) matches or exceeds the band gap energy E_g, of the semiconductor photocatalyst, an electron is promoted from the filled valence band into the empty conduction band leaving a hole behind. Depending on many factors, the photogenerated pairs (excited-state conduction-band electrons and valence-band holes) can undergo different fates. They can: (1) recombine and dissipate the input energy as heat; or (2) get trapped in metastable surface states; or (3) induce redox reactions with electron donors and electron acceptors adsorbed on the semiconductor surface, or within the surrounding electrical double layer of the charged particles. The possibility of driving redox reactions is of great interest; in fact, the valence-band holes are powerful oxidants (+1.0 to +3.5 V vs. NHE depending on the semiconductor and pH), while the conduction-band electrons are good reductants (+0.5 to −1.5 V vs. NHE). On this ground, the main difference between a traditional thermal catalyst

Correspondence concerning this article should be addressed to V. Augugliaro at augugliaro@dicpm.unipa.it.

and a photocatalyst is that the first one is always active *per se* while the second one turns active only when irradiated.

For real processes of polluted water remediation, the features of the "optimum" photocatalyst are the classical ones required to thermal catalysts (high-activity, stability, selectivity, low-cost, and so on). In addition, however, because the photocatalytic process needs a radiation source, the photocatalyst would have narrow band gap in order to use the most cheap radiation source, that is, solar light. Various semiconductor materials (for example, TiO_2, ZnO, Fe_2O_3, CdS, ZnS, and so on) have been tested as oxidation photocatalysts. However, as result of different problems mainly related to the photocatalyst stability under irradiation in water, it is generally accepted[8–11] that TiO_2, in anatase form, is the most reliable material for wastewater treatment. TiO_2 shows low-cost, high-photostability and activity; aqueous suspensions of this semiconductor can be activated by radiation with wavelength lower than 380 nm and, in this situation, a lot of redox reactions can occur at the catalyst surface.

Even if heterogeneous photocatalysis is considered greatly unselective[12] since very few species are refractory to photocatalytic oxidation, this technology has been also checked as a synthetic route. Some examples are represented by selective cyclization of amino acids in deaerated suspensions,[13] and photooxidation of cyclohexane yielding cyclohexanol and cyclohexanone as primary oxidation products.[14,15] Yet, toluene, methylcyclohexane, cyclohexane and ethylbenzene were selectively oxidized in aqueous TiO_2 suspensions,[16] while in gas phase[17] aldehydes and ketons were produced in high-yields from the corresponding primary and secondary alcohols. Recently, functionalizations of heterocyclic bases were performed by means of TiO_2 and visible light,[18] and one-pot photocatalytic synthesis of dihydropyrazine from ethylenediamine and propylene glycol was also carried out.[19] Deaerated suspensions of TiO_2 in ethanol and acetonitrile mixtures were lately used for the carbonylation of p-nitrotoluene to carbamate with high-selectivities.[20]

The increasing attention devoted to environment is not, however, limited only to its remediation; the stringent environmental limitations for chemical processes are driving the researchers all over the world to find new green syntheses performed in solvent-free reactors or in green solvents, as water or supercritical CO_2, and to avoid the use of heavy metals as catalysts, since they have a high environmental impact. In particular the development of green processes in the synthesis of hydroxylated aromatic species is of great concern as these compounds are used in pharmaceutical, food and cosmetic industries.

The photocatalytic oxidation of aromatic compounds has been largely investigated with the aim of finding the best operative conditions for their elimination from water and air. The kinetics and mechanisms of photocatalytic processes eventually determining the complete oxidation of these dangerous compounds have been studied paying a particular attention to the detection of stable intermediate products.[21–28] It has been found that concurrently with the pathway giving rise to the partial oxidation of the aromatic ring and then to the production of stable species, another reaction pathway generally takes place, that is, the direct mineralization of substrate to CO_2 through a series of adsorbed intermediates, that do not desorb from the catalyst surface toward the bulk of solution,[21,22,26] and, therefore, cannot be identified by analyzing the solution. By observing the first intermediates produced by a large number of aromatic compounds oxidized using different kinds of TiO_2 and experimental conditions, it was recently proved that the $HO^{\cdot}$ radical, the major species responsible of partial oxidation, enters selectively the aromatic ring in *ortho*- and *para*-positions in the presence of an electron donor group (EDG), while the absence of an EDG determines the unselective $HO^{\bullet}$ attack in all the three possible positions of the ring.[21,22]

In this work, the photocatalytic oxidation of nitrobenzene and phenylamine carried out in oxygenated aqueous suspension of commercial TiO_2 specimen in a batch photoreactor has been investigated as a synthetic route able to produce monohydroxylated aromatic compounds. On this ground, the duration of all the photoreactivity runs has been limited to irradiation times for which only one oxidative attack to the starting substrate occurred. This investigation has been aimed to verify the occurrence of two parallel oxidative processes, one partial and the second total, which operate from the start of aromatic compounds degradation, and to quantitatively model the kinetics of these processes. The identification of intermediate oxidation products and their quantitative determination have been used both for obtaining information on the likely oxidation pathways and for modeling the kinetics of substrate disappearance and intermediates production. It is important to outline that the reacting system gets very complex at high irradiation times, due to the occurrence of additional series-parallel reactions involving the different oxidation products of substrate, and, therefore, the kinetic model here proposed is valid only for the initial range.

Experimental

The used experimental setup has been elsewhere described in detail.[22] A Pyrex batch photoreactor of cylindrical shape with immersed lamp, containing 0.5 L of aqueous suspension, was used to perform the reactivity experiments. The photoreactor was provided with ports in its upper section for the inlet and outlet of gases and for sampling. A magnetic stirrer guaranteed a satisfactory suspension of the photocatalyst and the uniformity of the reacting mixture. A 125 W medium pressure Hg lamp (Helios Italquartz, Italy) axially positioned within the photoreactor was cooled by water circulating through a Pyrex thimble; the temperature of the suspension was about 300 K. The radiation energy impinging on the suspension had an average value of 10 mW cm^{-2}. It was measured by using a radiometer UVX Digital, at $\lambda =$ 360 nm.

For all the runs, TiO_2 Merck (~100% anatase, BET surface area: ca. 10 $m^2\ g^{-1}$) was used as photocatalyst with an amount of 0.4 g l^{-1}; it was checked that with this amount all the suspension was irradiated and the transmitted photon flow was negligible. The initial pH of the suspension was 6.5, that is, the natural one. Nitrobenzene and phenylamine were reagent grade (Sigma Aldrich).

Experiments for determining the amount of substrate adsorbed onto TiO_2 surface at room temperature lasted 1 h; this time was sufficient for achieving steady-state conditions. The substrate concentrations were measured before the addition of the catalyst and at the end of the run; these values allowed to calculate the amounts of adsorbed substrate.

Different photoreactivity runs were carried out with substrate initial concentration in the 200–800 μM range.

The suspension, once prepared, was saturated by bubbling O_2 at atmospheric pressure for 1 h before turning on the lamp. Oxygen was continuously bubbled in the course of the runs that lasted 1.5 h. Samples for analyses were withdrawn at fixed intervals of time; the catalyst was immediately separated from the aqueous solution by filtering through 0.45 μm Millex Millipore filters.

The substrates and all the mono-hydroxylated species produced during the irradiation time were analyzed with a HPLC Beckman Coulter (System Gold 126 Solvent Module and 168 Diode Array Detector), equipped with a Luna 5 μ Phenyl-Hexyl column (250 mm long $\times$ 2 mm i.d.); the eluent consisted of methanol, acetonitrile and an aqueous KH_2PO_4 solution in different ratios depending on the analyzed substrate. The flow rate was 0.2 mL min^{-1}, and the identification was carried out by comparison with authentical samples, purchased from Sigma-Aldrich.

Total organic carbon (TOC) analyses were carried out by using a 5000A Shimadzu TOC analyser; for each sample six analyses were performed; the mean value was calculated after rejecting the highest and the lowest values. These analyses aimed to determine the amount of organic carbon mineralized to CO_2.

Results

The results obtained from the adsorption runs showed a relevant decrease of nitrobenzene concentration (ca. 8% mol), while as far as phenylamine is concerned no detectable adsorption was observed.

Figures 1 and 2 show experimental results obtained from some representative runs carried out with nitrobenzene and phenylamine, respectively. The figures report the concentration values of substrate, of all the detected monohydroxylated intermediates, and of the mineralized organic carbon (determined from the TOC values) versus the irradiation time. It is worth noting that the values of the mineralized carbon concentration reported in Figures 1 and 2 are obtained by dividing by 6 the measured TOC values in order to be comparable with the concentrations of oxidized compounds that contain 6 carbon atoms. By considering all the identified reaction products (monohydroxylated intermediates and CO_2), for all the substrate initial concentrations, the carbon mass balance was clearly satisfied in the first hour of irradiation; at irradiation times in the 1–1.5 h a modest loss of carbon in the mass balance can be noted, probably due to the starting of production of noticeable amounts of polyhydroxylated aromatic species and open-ring compounds. For irradiation times higher than 1.5 h, the production of polyhydroxylated aromatic species and open-ring compounds gets very important so that only the data obtained in the first 1.5 h have been used for the kinetic modeling.

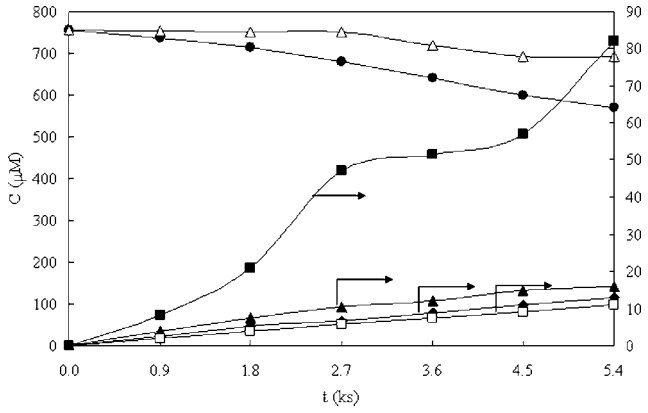

Figure 1. Experimental results of a representative nitrobenzene oxidation run.

Concentration values of: ●, nitrobenzene; ▲, 2-nitrophenol; □, 3-nitrophenol; ◆, 4-nitrophenol; ■, and mineralized carbon. △, mass balance on carbon.

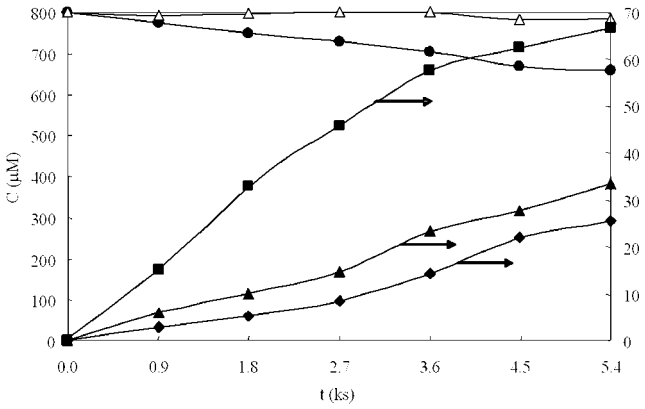

Figure 2. Experimental results of a representative phenylamine oxidation run.

Concentration values of: ●, phenylamine; ▲, 2-hydroxyphenylamine; ◆, 4-hydroxyphenylamine; and ■, mineralized carbon. △, mass balance on carbon.

Figure 3 shows the nitrobenzene and phenylamine concentration values vs. irradiation time for runs carried out at different initial concentration of substrate. It may be noted that nitrobenzene exhibits a photoreactivity higher than that of phenylamine; moreover for both substrates the reaction rate increases by decreasing the initial concentration as it is typical of photocatalytic oxidations.[29]

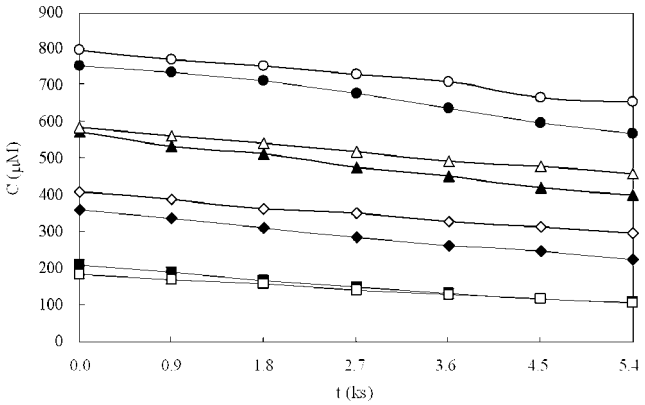

Figure 3. Nitrobenzene (full symbols) and phenylamine (empty symbols) concentration values vs. the irradiation time.

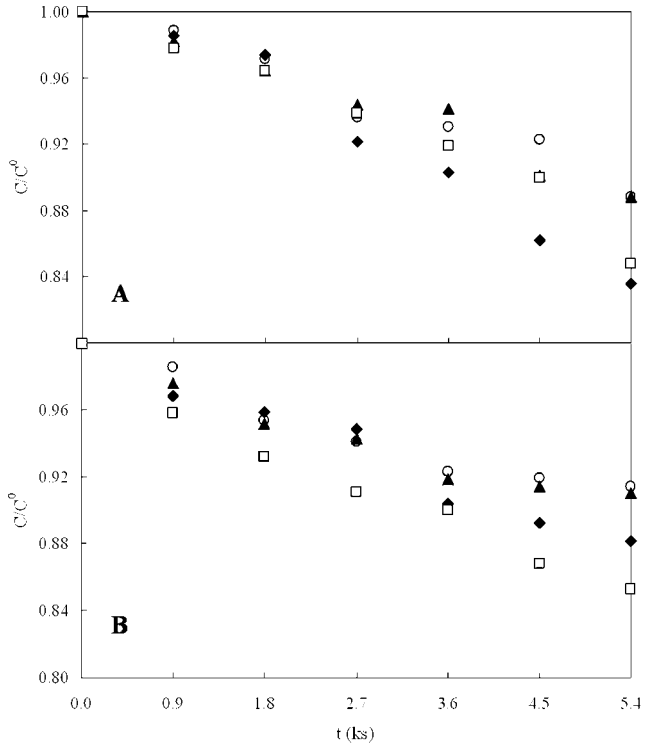

Figure 4. TOC evolution with irradiation time. (A) Initial TOC concentration for nitrobenzene: □, 15.5 mg l^{-1}.; ◆, 26.8 mg l^{-1}; ▲, 39.3 mg l^{-1}; ○, 52.9 mg l^{-1}, and (B) Initial TOC concentration for phenylamine: □, 19.0 mg l^{-1}.; ◆, 31.2 mg l^{-1}; ▲, 45.5 mg l^{-1}; ○, 55.8 mg l^{-1}.

Figure 4 shows the TOC evolution during the oxidation of nitrobenzene (A) and phenylamine (B), respectively. It must be reported that TOC analyses, even if repeated six times on the same samples for each run, generally give quite scattered values which, however, furnish reliable information when considered jointly. Assuming that no volatile organic compounds were formed or their amount was negligible, the decrease of TOC concentration may be ascribed only to CO_2 production. Indeed, CO_2 was detected from the starting of irradiation and its concentration increased by increasing the reaction time. The substrate mineralized in 1.5 h was in 8–16% mol range.

Figure 5 shows the total amounts of the produced monohydroxy derivatives during nitrobenzene (A), and phenylamine (B) oxidation for runs carried out at different initial concentrations of substrate. It may be noted that the concentrations of these partial oxidation products increase by increasing the irradiation time and the initial substrate concentrations. In the case of nitrobenzene oxidation the monohydroxy derivatives concentration reaches a constant value in the run carried out with the lowest initial concentration (see Figure 5a); it is likely that in this case the further photooxidation reactions become significant. While the monohydroxy derivatives were produced in major extent from phenylamine (Figure 5b), the production of CO_2 was higher for nitrobenzene (Figure 4a).

Discussion

Reaction pathway

The observation of the experimental results clearly indicates that from the start of irradiation two parallel pathways are operating on the substrate: (1) complete mineralization with production of CO_2; and (2) formation of monohydroxylated species released into the bulk of the solution. The transformation of substrate to CO_2 occurs through intermediate species that remain adsorbed onto the irradiated TiO_2 surface, and, therefore, cannot be revealed by analyzing the solution. By investigating the phenol degradation in aqueous suspensions of TiO_2, Salaices et al.[28] proposed a mechanism which involves series-parallel reactions, that is, simultaneous in-series progressive incorporation of $HO^{\bullet}$ groups in the phenol and the phenolic derived species, and parallel oxidation pathways producing CO_2. By comparing the adsorption and photoreactivity results obtained with nitrobenzene and phenylamine, it may be stated that the nature of the substituent group present in the aromatic ring strongly influences: (1) the substrate adsorption onto the TiO_2 surface in the dark, and (2) the position of the hydroxyl group entering the aromatic ring. Phenylamine, with an electron donor group (EDG) as NH_2, reveals a negligible adsorption while a noticeable adsorption is shown by nitrobenzene with an electron

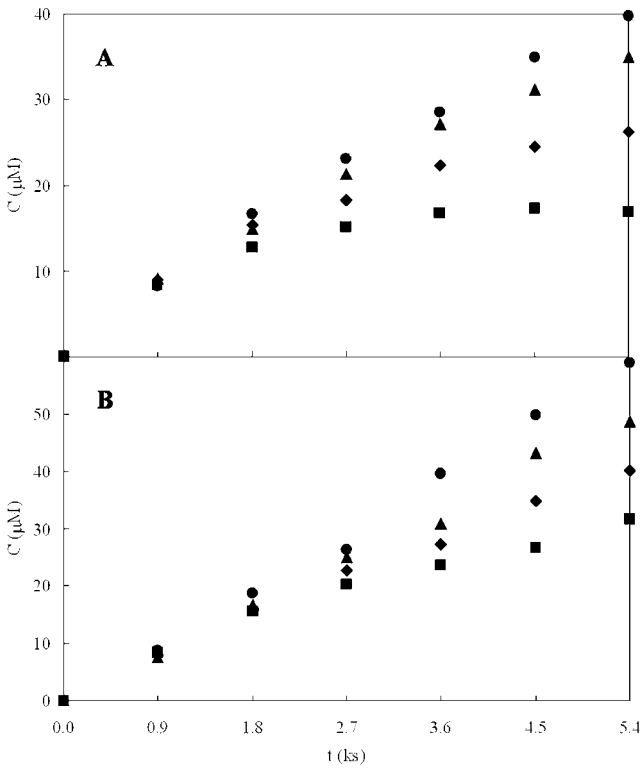

Figure 5. Monohydroxy derivatives (*ortho* + *meta* + *para*) formed during nitrobenzene (A) and phenylamine (B) photocatalytic oxidation. Initial nitrobenzene concentrations: ■, 180 μM; ◆, 410 μM; ▲, 590 μM; ●, 800 μM. Initial phenylamine concentrations: ■, 210 μM; ◆, 360 μM; ▲, 570 μM; ●, 760 μM.

withdrawn group (EWG) as NO_2. The additional electron density, induced in the aromatic ring by the presence of NH_2, is not beneficial for the molecule adsorption while the presence of NO_2, by reducing the electron density of the aromatic ring, favors the adsorption of the molecule onto the catalyst surface.

It is generally accepted that in heterogeneous photocatalysis the oxidation reactions occur through a mechanism involving HO• radicals.[1–8] The oxidation of the radical intermediates arising from the addition of a hydroxyl radical to the aromatic ring of the substrates could occur in different ways: (1) by means of another hydroxyl radical for hydrogen abstraction; or (2) by means of electron transfer followed by proton elimination. As concerning the selectivity of the HO• radical attack to the aromatic ring in *ortho*-, *meta*- and *para*-positions, the attack seems to be strongly dependent on the kind of substituent. The literature regarding the intermediates found during the photocatalytic oxidation of substituted aromatic compounds confirms this finding. In particular Augugliaro et al.[30] reported the formation of 1-amino, 2-hydroxy benzene and 1-amino, 4-hydroxy benzene during the photocatalytic oxidation of phenylamine. Bhatkhande et al.[25] degraded nitrobenzene using concentrated solar radiation, and detected all the three monohydroxy derivatives as intermediates.

The data obtained in this work indicate that with nitrobenzene all the three monohydroxy derivatives are obtained (average molar percentages: 29% *ortho*, 34% *meta*, 37% *para*), while with phenylamine the main monohydroxylated compounds are *ortho*- and *para*-isomers (average molar percentages: 60% *ortho*, 40% *para*) being the *meta*-isomer practically absent. On the basis of these results, it may be confirmed that the heterogeneous photocatalytic oxidation of benzene derivatives is a selective reaction. In the presence of an EDG almost only the *ortho*- and *para*-isomers are formed while, when an EWG is present,[21,22] all the three monohydroxy derivatives are obtained.

Scheme 1 shows the hypothesized reaction mechanisms, involving the parallel reactions of monohydroxylation of the aromatic ring and production of CO_2 (obtained from the oxidation of unidentified adsorbed intermediates).

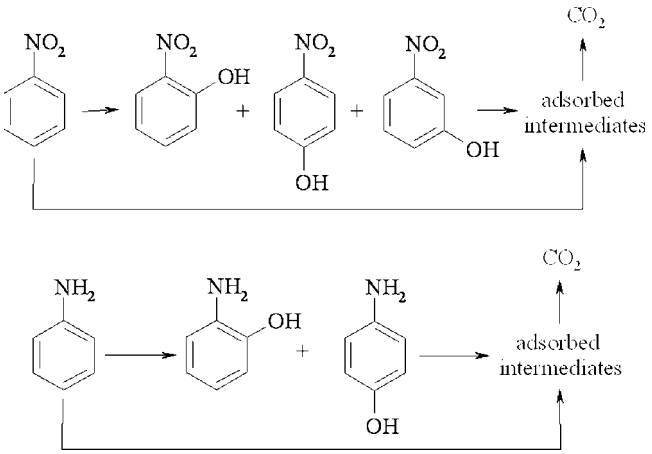

Scheme 1. Reaction mechanisms of nitrobenzene and phenylamine photocatalytic oxidation.

Kinetic modeling

In order to model the photoreactivity results, the assumption is made that all the elementary reactions of phenylamine and nitrobenzene oxidation, both partial and total, occur on the catalyst surface and involve adsorbed species, which can interact with hydroxyl groups. The rate-determining step of the photooxidation process on the catalyst surface is hypothesized to be the second-order reaction between HO• radical and aromatic molecule adsorbed onto the catalyst surface. This simple model is commonly used to analyze the kinetics of photocatalytic reactions and it generally provides a satisfactory prediction of the progress of species concentration in liquid[31–33] or gas[34] phase.

Different types of sites are hypothesized to exist onto the catalyst surface. As the adsorbed oxygen acts as an electron trap, thus, hindering the electron-hole recombination, the HO• radical concentration depends on the fractional sites coverage by O_2. Moreover, the occurrence for phenylamine and nitrobenzene of two parallel pathways, that is, partial oxidation and mineralization, suggests that the adsorption sites responsible of these pathways must possess distinguishing features, that is, different natures. On this ground the kinetic modeling of photoreactivity results is here made by assuming that three different types of site exist on the catalyst surface. The first type is able to adsorb oxygen, the second one adsorbs the substrates by producing monohydroxylated species, and the third one adsorbs the substrates and their intermediate products by eventually producing their mineralization.

In this hypothesis the disappearance rate of substrate for second-order surface reactions in parallel (monohydroxylation and mineralization) may be written in terms of Langmuir-Hinshelwood kinetics as

$$(-r_S) \equiv -\frac{1}{S}\frac{dN_S}{dt} = k_1\theta_{Ox}\theta_1 + k_2\theta_{Ox}\theta_2 \tag{1}$$

in which S is the specific surface area of the catalyst, N_S the substrate moles, t the irradiation time and θ_{Ox} the fractional site coverage of oxygen. k_1 and k_2 are the second-order rate constants, and θ_1 and θ_2 the fractional site coverages of the substrate evolving to monohydroxy derivatives, and of the substrate that is directly oxidized to CO_2, respectively.

By considering that the monohydroxy intermediates, once formed, compete with the starting substrates for the adsorption on the mineralizing sites, the fractional site coverages, given by the Langmuir relationship, are

$$\theta_{ox} = \frac{K_{ox}C_{ox}}{1 + K_{ox}C_{ox}} \tag{2}$$

$$\theta_1 = \frac{K_{MH}C_S}{1 + K_{MH}\left(C_S + \sum_I C_I\right)} \tag{3}$$

$$\theta_2 = \frac{K_{Min}C_S}{1 + K_{Min}\left(C_S + \sum_I C_I\right)} \tag{4}$$

where C_{ox}, C_S and C_I are the oxygen, the substrates and the monohydroxy derivatives concentrations in the aqueous

Table 1. Equilibrium Adsorption Constants and Kinetic Constants for Nitrobenzene and Phenylamine Photocatalytic Partial Oxidation (K_{MH}, k^{I}) and Mineralization (K_{Min}, k^{II}) together with the Corresponding 90% Confidence Intervals

	Nitrobenzene	Phenylamine
K_{MH} (mM^{-1})	8.05 ± 1.02	1.10 ± 0.13
K_{Min} (mM^{-1})	2.13 ± 0.32	2.02 ± 0.28
$k^{I} \cdot 10^{9}$ (mol m^{-2} s^{-1})	5.03 ± 0.62	6.05 ± 0.51
$k^{II} \cdot 10^{9}$ (mol m^{-2} s^{-1})	6.10 ± 0.77	5.90 ± 0.95

phase, whereas K_{ox}, K_{MH} and K_{Min} are the equilibrium adsorption constants of oxygen, and of substrate on monohydroxylating and mineralizing sites, respectively. In writing Eqs. 3 and 4 the assumption is made that the values of equilibrium adsorption constants of the substrates and monohydroxy derivatives are similar,[31–33] both for the hydroxylation site and for the mineralization one.

Because all the experiments were carried out in a batch reactor by continuously bubbling oxygen into the liquid phase, the fractional site coverage of oxygen is constant during the occurrence of the run. By substituting Eqs. 3 and 4 in Eq. 1, one obtains

$$-\frac{V}{S}\frac{dC_S}{dt} = k^{I}\frac{K_{MH}C_S}{1+K_{MH}\left(C_S+\sum_I C_I\right)} + k^{II}\frac{K_{Min}C_S}{1+K_{Min}\left(C_S+\sum_I C_I\right)} \quad (5)$$

where V is the reaction volume, $k^{I} = k_1\theta_{Ox}$, and $k^{II} = k_2\theta_{Ox}$.

The production rate of intermediates can be expressed as follows

$$\frac{V}{S}\frac{d\sum_I C_I}{dt} = k^{I}\frac{K_{MH}C_S}{1+K_{MH}\left(C_S+\sum_I C_I\right)} - k^{II}\frac{K_{Min}\sum_I C_I}{1+K_{Min}\left(C_S+\sum_I C_I\right)} \quad (6)$$

The production rate of CO_2, normalizing its concentration to the substrates one, can be expressed as

$$\frac{V}{S}\frac{d(C_{CD}/6)}{dt} = k^{II}\frac{K_{Min}\left(C_S+\sum_I C_I\right)}{1+K_{Min}\left(C_S+\sum_I C_I\right)} \quad (7)$$

where C_{CD} is the carbon dioxide concentration. By substituting $C_{CD}/6$ with C', the global molar balance can be described by the following relationship

$$C_{S,0} = C_S + \sum_I C_I + C' \quad (8)$$

$$C_S + \sum_I C_I = C_{S,0} - C' \equiv y \quad (9)$$

in which $C_{S,0}$ is the initial substrate concentration. By substituting Eq. 9 in Eq. 7, the following differential equation is obtained

$$-\frac{V}{S}\frac{dy}{dt} = k^{II}\frac{K_{Min}y}{1+K_{Min}y} \quad (10)$$

Integration of Eq. 10 with the limiting conditions that $y = C_{S,0}$ at $t = 0$ and $y = C_{S,0}-C'$ at $t = t$ gives

$$t = \frac{V}{S}\frac{1}{k^{II}K_{Min}}\left(\ln\frac{C_{S,0}}{C_{S,0}-C'} + K_{Min}C'\right) \quad (11)$$

By applying a least-square best fitting procedure of Eq. 11 to all the experimental data of C' vs. t, the values of k^{II} and K_{Min} ($R^2 > 0.95$) for nitrobenzene and phenylamine have been obtained. This nonlinear fit was carried out by using the curve-fitting function available in Mathematica version 4 (Wolfram Media). These values are reported in Table 1 together with the 90% confidence intervals. In order to compare the experimental data with the kinetic model (Eq. 11) which gives t as a variable dependent on C', for some representative runs Figure 6 shows the experimental values of t vs. C'. The lines drawn through the experimental points represent Eq. 11, in which the fitted parameters have been substituted; a satisfactory fitting of the model to the experimental data may be noted. Moreover, the obtained results suggest that the mineralization pathway is similar for both substrates. In fact the lines indicating the kinetic model are very close each other, thus, indicating that the nature of substituent group does not influence the mineralization reaction.

To determine k^{I} and K_{MH} Eq. 10 has been divided for Eq. 5 giving rise to the following relation

$$\frac{dy}{dC_S} = \frac{Ay(1+K_{MH}y)}{C_S[(1+K_{Min}y)+A(1+K_{MH}y)]} \quad (12)$$

where $A = (K_{Min}k^{II})/(K_{MH}k^{I})$.

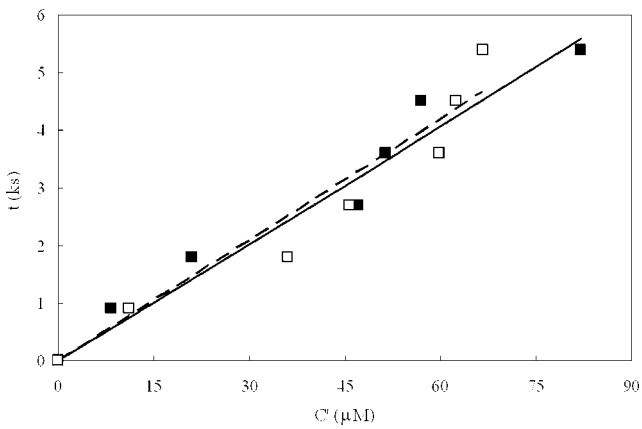

Figure 6. Experimental values of irradiation times vs. C' (≡ $C_{CD}/6$): ■, nitrobenzene (initial concentration: 760 μM); □, phenylamine (initial concentration: 800 μM).

The continuous and dotted lines represent the kinetic model (Eq. 11) for nitrobenzene and phenylamine runs, respectively.

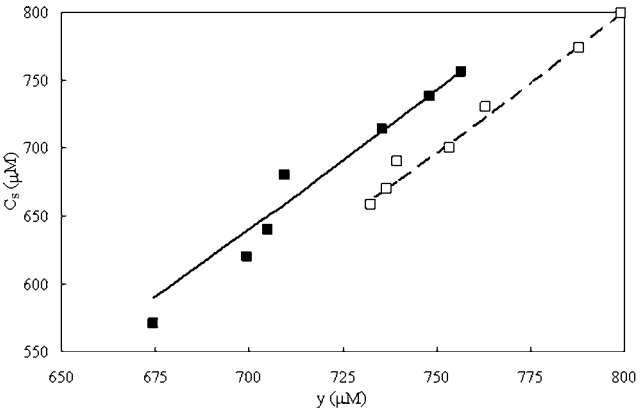

Figure 7. Experimental values of C_S vs. y (defined in Eq. 9): ■, nitrobenzene (initial concentration: 760 μM); □, phenylamine (initial concentration: 800 μM).

The continuous and dotted lines represent the kinetic model (Eq. 13) for nitrobenzene and phenylamine runs, respectively.

By integrating Eq. 12 with the limit conditions that $y = y^0$ for $C_S = C_{S,0}$ and $y = y$ for $C_S = C_S$, one obtains the following equation

$$\ln\left(\frac{C_{S,0}}{C_S}\frac{y}{y^0}\right) = \frac{K_{Min}}{AK_{MH}}\ln\frac{1+K_{MH}y^0}{1+K_{MH}y} + \frac{1}{A}\left(\frac{y^0}{y}\frac{1+K_{MH}y}{1+K_{MH}y^0}\right) \tag{13}$$

Substituting the values of k^{II} and K_{Min} in Eq. 13, the least-square best fitting procedure for all the runs, at different initial concentrations, yielded the values of k^I and K_{MH} for nitrobenzene and phenylamine. They are reported in Table 1 together with the 90% confidence intervals. For some representative runs, Figure 7 reports the values of C_S as a function of y; the lines drawn through the experimental points represent the kinetic model (Eq. 13) in which the fitted parameters have been substituted; also in this case a satisfactory fitting of the model to the experimental data may be noted. The results indicate that as far as phelylamine is concerned the production of monohydroxy derivatives is higher than nitrobenzene, suggesting that the presence of either ED or EW substituent groups influence not only the regioselectivity of hydroxyl radical, but also the relative amount of the monohydroxy derivatives.

The data reported in Table 1 indicate that the value of the equilibrium adsorption constant of nitrobenzene on hydroxylating sites is one order of magnitude higher than that of phenylamine, on the contrary the values of equilibrium adsorption constants on mineralizing sites are quite similar. By considering that these values derive from a kinetic modeling procedure, this finding would suggest that the mineralizing sites are nonspecific toward the organic molecules, while the sites able to perform partial oxidation need a molecule with specific features, as it is the case for nitrobenzene which shows a measurable adsorption in the dark differently from phenylamine.

The values of kinetic constant (see Table 1) for partial oxidation and mineralization both of nitrobenzene and phenylamine are all of the same order of magnitude. With the same limitation above expressed, this finding suggests that the oxidative events occurring on the catalyst surface, once the organic molecules occupy the active sites, are all of the same nature, independently of the specific active site and adsorbed aromatic compound.

Conclusion

The photocatalytic oxidation of nitrobenzene and phenylamine in aqueous TiO_2 suspension proceeds through two parallel reaction pathways: the first produces monohydroxy derivatives which desorb from the catalyst surface, and the second CO_2 from adsorbed intermediates which are not released to the liquid phase. The Langmuir-Hinshelwood kinetic model provides satisfactory results for all the initial concentrations, but it is strictly suitable in the initial stage of the photoprocess when the reaction products are only monohydroxy derivatives. Further extended oxidation of the intermediates causes a failure of this model which does not consider the production of polyhydroxy derivatives and open-ring products.

Acknowledgment

Financial support by MIUR (Rome) is gratefully acknowledged.

Literature Cited

1. Schiavello M. *Photoelectrochemistry, Photocatalysis, and Photoreactors. Fundamentals and Developments*. Dordrecht: Reidel; 1985.
2. Pelizzetti E, Serpone N. *Homogeneous and Heterogeneous Photocatalysis*. Dordrecht: Reidel; 1986.
3. Schiavello M. *Photocatalysis and Environment. Trends and Applications*. Dordrecht: Kluwer; 1988.
4. Serpone N, Pelizzetti E. *Photocatalysis, Fundamentals and Applications*. New York: Wiley; 1989.
5. Ollis DF, Al-Ekabi H. *Photocatalytic Purification and Treatment of Water and Air*. New York: Elsevier; 1993.
6. Hoffmann MR, Martin ST, Choi W, Bahnemann DW. Environmental applications of semiconductor photocatalysis. *Chem Rev*. 1995;95: 69–96.
7. Schiavello M. *Heterogeneous Photocatalysis*. Chichester: Wiley; 1997.
8. Fujishima A, Hashimoto K, Watanabe T. TiO_2 *Photocatalysis. Fundamentals and Applications*. Tokyo: BKC, Inc; 1999.
9. Fujishima A, Rao TN, Tryk DA. Titanium dioxide photocatalysis. *J Photochem Photobiol C: Photochem Rev*. 2000;1:1–21.
10. Yasumori A, Shinoda H, Kameshima Y, Hayashi S, Okada K. Photocatalytic and photoelectrochemical properties of TiO_2-based multiple layer thin film prepared by sol-gel and reactive-sputtering methods. *J Mat Chem*. 2001;4:1253–1257.
11. Loddo V, Addamo M, Augugliaro V, Palmisano L, Schiavello M, Garrone E. Optical properties and quantum yield determination in photocatalytic suspensions. *AIChE J*. 2006;52:2565–2574.
12. Cabrera M, Alfano O, Cassano A. Novel reactor for photocatalytic kinetic studies. *Ind Eng Chem Res*. 1994;33:3031–3042.
13. Ohtani B, Pal B, Ikeda S. Photocatalytic organic syntheses: selective cyclization of amino acids in aqueous suspensions. *Catal Surv Asia*. 2003;7:165–176.
14. Almquist CB, Biswas P. The photo-oxidation of cyclohexane on titanium dioxide: an investigation of competitive adsorption and its effects on product formation and selectivity. *Appl Catal A: Gen*. 2001;214:259–271.
15. Sahle-Demessie E, Gonzalez M, Wang Z, Biswas P. Synthesizing alcohols and ketones by photoinduced catalytic partial oxidation of hydrocarbons in TiO_2 film reactors prepared by three different methods. *Ind Eng Chem Res*. 1999;38:3276–3284.

16. Gonzalez MA, Howell SG, Sikdar S. Photocatalytic selective oxidation of hydrocarbons in the aqueous phase. *J Catal*. 1999;183:159–162.
17. Pillai UR, Sahle-Demessie E. Selective oxidation of alcohols in gas phase using light-activated titanium dioxide. *J Catal*. 2002;211:434–444.
18. Caronna T, Gambarotti C, Palmisano L, Punta C, Recupero F. Sunlight induced functionalisation of some heterocyclic bases in the presence of polycrystalline TiO_2. *Chem Commun*. 2003;18:2350–2351.
19. Subba Rao KV, Srinivas B, Subrahmanyam M, Prasad AR. A novel one step photocatalytic synthesis of dihydropyrazine from ethylenediamine and propylene glicol. *Chem Commun*. 2000;16:1533–1534.
20. Maldotti A, Amadelli R, Samiolo L, Molinari A, Penoni A, Tollari S, Cenini S. Photocatalytic formation of a carbamate through ethanol-assisted carbonylation of p-nitrotoluene. *Chem Commun*. 2005;13:1749–1751.
21. Palmisano G, Addamo M, Augugliaro V, Caronna T, García-López E, Loddo V, Palmisano L. Influence of the substituent on selective photocatalytic oxidation of aromatic compounds in aqueous TiO_2 suspensions. *Chem Commun*. 2006;1012–1014.
22. Palmisano G, Addamo M, Augugliaro V, Caronna T, Di Paola A, García-López E, Loddo V, Marcì G, Palmisano L, Schiavello M. Selectivity of hydroxyl radical in the partial oxidation of aromatic compounds in heterogeneous photocatalysis. *Catal Today*. 2007; in press. Doi: 10.1016/J.cattod.2007.01.026.
23. Peiró AM, Ayllón JA, Peral J, Doménech X. TiO_2-photocatalyzed degradation of phenol and ortho-substituted phenolic compounds. *App Catal B: Environ*. 2001;30:359–373.
24. Parra S, Olivero J, Pacheco L, Pulgarin C. Structural properties and photoreactivity relationships of substituted phenols in TiO_2 suspensions. *Appl Catal B: Environ*. 2003;43:293–301.
25. Bhatkhande DS, Pangarkar VG, Beenackers AACM. Photocatalytic degradation of nitrobenzene using titanium dioxide and concentrated solar radiation: chemical effects and scaleup. *Water Res*. 2003;37:1223–1230.
26. Marcì G, Addamo M, Augugliaro V, Coluccia S, García-López E, Loddo V, Martra G, Palmisano L, Schiavello M. Photocatalytic oxidation of toluene on irradiated TiO_2: comparison of degradation performance in humidified air, in water and in water containing a zwitterionic surfactant. *J Photochem Photobiol A: Chem*. 2003;160:105–114.
27. Piccinini P, Minero C, Vincenti M, Pelizzetti E. Photocatalytic mineralization of nitrogen-containing benzene derivatives. *Catal Today*. 1997;39:187–195.
28. Salaices M, Serrano B, de Lasa HI. Photocatalytic conversion of phenolic compounds in slurry reactors. *Chem Eng Sci*. 2004;59:3–15.
29. Augugliaro V, Loddo V, Marcì G, Palmisano L, López-Muñoz MJ. Photocatalytic oxidation of cyanides in aqueous titanium dioxide suspensions. *J Catal*. 1997;166:272–283.
30. Augugliaro V, Bianco Prevot A, Loddo V, Marcì G, Palmisano L, Pramauro E, Schiavello M. Photodegradation kinetics of aniline, 4-ethylaniline, and 4-chloroaniline in aqueous suspension of polycrystalline titanium dioxide. *Res Chem Intermed*. 2000;26:413–426.
31. Turchi CS, Ollis DF. Mixed reactant photocatalysis - intermediates and mutual rate inhibition. *J Catal*. 1989;112:483–496.
32. Augugliaro V, Cavallero L, Marcì G, Palmisano L, Pramauro E. Influence of operational variable on the photodegradation kinetics of monuron in aqueous titanium dioxide dispersions. *Stud Surf Sci Catal*. 1994;82:713–720.
33. Gora A, Toepfer B, Puddu V, Li Puma G. Photocatalytic oxidation of herbicides in single-component and multicomponent systems: reaction kinetics analysis. *Appl Catal B: Environ*. 2006;65:1–10.
34. Ibrahim H, de Lasa H. Kinetic modeling of the photocatalytic degradation of air-borne pollutants. *AIChE J*. 2004;50:1017–1027.

Manuscript received Nov. 20, 2006, and revision received Jan. 16, 2007.